Short Communication

Advanced Electrocatalytic Performance of Activated Carbon Prepared from Asphalt

Huiying Wang[1,2], Peifeng Cheng[1,2,*] and Yiqi Wang[1,2]

[1] College of Civil Engineering, Northeast Forestry University, Harbin City, Heilongjiang Province, 150000, P.R. China
[2] School of Civil Engineering and Civil Engineering, Heilongjiang Institute of Technology, Harbin City, Heilongjiang Province, 150000, P.R. China
[*]E-mail: peifengcheng@tom.com

In the present work, nitric and sulfuric acids were used for the chemical conversion of asphalt to activated carbon (AC) powder. An extremely high cation exchange capacity was obtained under the following conditions: no airflow rate injection and ratio of acid/asphalt, 30 wt%. When the pH was *ca.* 3 (initial pH range of 3 to 10), a stable zero point of charge was observed for the obtained product. The final composites showed the following integrated advantages: the effectiveness of the oxygen reduction reaction (ORR) active sites and the excellence of the electrical conductivity. The final material can be used not only as an effective metal-free electrode material but also as a competitive substitute material for the recently discovered Pt/C catalyst given the remarkable electrochemical activity toward ORR observed under alkaline conditions.

1. INTRODUCTION

Proton exchange membrane fuel cells (PEMFCs) have been recognized as a highly efficient and competitive energy conversion system for not only stationary but also mobile applications. To successfully introduce fuel cells into the market, the development of a low-cost, durable and highly active cathode electrocatalyst is urgently required. Currently, the state-of-the-art cathode electrocatalysts consist of platinum metal or its alloys with carbon black as support [1-4]. Unfortunately, the energy conversion efficiency of such fuel cells is typically limited mainly by the slow kinetics for the oxygen reduction reaction (ORR) even on Pt catalysts [5-8]. In addition, Pt is not only expensive but also of low abundance. The development of substitute low-cost electrocatalysts for the cathode side of PEM fuel cells has gained substantial attention in the past few decades. Metal-

N_4 macrocycles, including Fe- and Co-porphyrins and -phthalocyanines, show desirable potential since they are highly active in the ORR [9-11]. However, this type of catalyst also suffers from a few disadvantages, with the most major disadvantage being the low stability under PEM fuel cell conditions; the poor stability results from problems associated with the production of H_2O_2 as a reactive intermediate, such as the degradation of the Nafion membrane, the leaching of Co and Fe, and the oxidation of the carbon support [12, 13]. Heat treatment or electropolymerization of carbon black-supported metalloporphyrins and phthalocyanines can partially compensate for the poor stability [14-20]. The partial or complete destruction of the macrocycle depends on the temperature of the heating treatment [21-24]. On the other hand, it has been reported that species such as FeN_4C_y and FeN_2C_x can form as active sites for the ORR [25-29]. Based on experimental and theoretical results, it can be concluded that much simpler iron, nitrogen, and carbon black compounds can be heated to form similar active sites without the need for macrocycles; such materials are promising candidates for use as a substitute catalyst for the cathode side in PEM fuel cells [30-34]. Unfortunately, the noble-metal-free electrocatalysts described above need to be improved due to their poor stability and activity in fuel cell applications.

Carbon materials have been recently used as catalysts and characterized for the purpose of ORR[35]. When appropriately treated, nearly all carbonaceous material from minerals or plants can be converted into activated carbon (AC). Based on the literature, successful conversion has been demonstrated for materials originating from plants and animals, including coconut shells [36], almond shells [37], olive stones [38], corncobs [39], and apricot stones [40]. Pereiras et al. [41] have proposed the selective modification of the surface chemistry for commercial-activated carbon (CAC) through thermal and chemical treatments without obviously changing its textural features. Moreover, the surface chemistry of the AC was found important in the dye adsorption behavior.

The preparation of AC from petroleum residues has been previously reported. The present work prepared AC using asphalt as a raw material. To obtain further understanding of the property of the active sites, an electrochemical study was carried out on the catalytic activity of the AC (produced from asphalt) for the ORR.

2. EXPERIMENTS

2.1. Preparation of activated carbon(AC)

AC was produced from asphalt as a raw material. A mixture of acid/asphalt with varying weight ratios of 20:1 to 60:1 was produced by adding concentrated sulfuric acid into this material. The mixtures were then vigorously agitated at a temperature range of 400-900 °C, with compressed air sparged throughout the solution. To promote the oxidation of the obtained AC, a small amount of concentrated nitric acid in the range of 3-10 mL was added into the mixed solution. Upon the completion of this reaction, the residual solid was washed several times using distilled water until a pH value of ca. 4 was reached. This was followed by increasing the pH value up to 7 through the addition

of a few drops of diluted NaOH (0.1 M). To remove any residual water, the mixed solution was left to dry for 60 min and then stored in a closed tight container prior to further use.

2.2. Instruments

Thermoanalytic experiments were carried out using a NETSCH STA449F3 thermobalance setup under N_2 atmosphere, with the following parameters: heating rate, 10 K/min; temperature range, 40–900 °C; and constant gas flow, 50 mL/min. A Vario EL III CHNOS elemental analyzer was used for the elemental determination of C, H, and N. Before the measurement of nitrogen sorption, the collected specimens were left to dry for 7 h at 150 °C. A Bruker D8 diffractometer was used to record the X-ray diffraction (XRD) patterns (reflection mode) between 2° and 80° with Cu Kα radiation.

2.3 Cation exchange capacity

A 4 g sample of the AC produced was mixed with 33 mL of 1 M sodium acetate solution, resulting in an exchange between the added sodium ions and the matrix cations. Subsequently, the sample was washed with 33 mL of isopropyl alcohol. A volume of 33 mL of ammonium acetate solution (1 M) was then added, which replaces the adsorbed sodium with ammonium. The concentration of displaced sodium was then determined by the CHNOS elemental analyzer.

2.4 Measurement of zero point of charge

A batch equilibrium technique was applied to determine the pH at the zero point of charge. Portions of the produced activated carbon powder (0.5 g) were introduced into a known volume (20 mL) of 0.1 M KNO_3 solution. Potassium nitrate (KNO_3) was selected as an inert electrolyte. The initial pH values of the KNO_3 solutions were adjusted to cover a range from 4.5 to 11.5 by adding 0.1 M of HNO_3 or KOH. The solutions were then allowed to equilibrate for 24 h in an isothermal shaker at 25 °C. Finally, the suspensions were filtered through filter paper, and the pH values were measured.

2.5. Electrochemical measurements

An IviumStat multichannel electrochemical analyzer in a three-electrode configuration was used to study the electrochemical activity of the as-prepared materials for the ORR. The working, reference and counter electrodes were a rotating disk electrode (RDE), saturated calomel electrode (SCE), and Pt wire, respectively. In terms of the rotating disk electrode (RDE) measurement, a glassy carbon electrode (GCE) was pre-treated by polishing and clean rinsing. This was followed by dispersal of the carbon specimen (5 mg) into a mixed solution of 0.7 mL of ethanol, 0.35 mL of deionized water, and 0.08 mL of Nafion (5 wt%). Linear sweep voltammetry measurements were carried out using the RDE at different rotating speeds ranging from 400 to 2025 rpm at a scan rate of 5 mV/s and at room temperature after purging O_2 for at least 30 min. Under the same conditions (except for a halved

loading of catalyst), a commercial 20 wt% Pt/C catalyst was also synthesized and analyzed for comparison. A ring-disk electrode with a Pt ring and glassy carbon disk functioned as the working electrode for the experiments using a rotating ring-disk electrode (RRDE) at a ring potential of 0.5 V, with the loading for the catalyst the same as that used in the RDE experiment. CV was carried out for a scan rate range of 20 mV/s and a potential range of 0.2-1.2 V. The Koutecky–Levich equations shown below were used to evaluate the transferred electron number (n).

3. RESULTS AND DISCUSSION

The ash density and content recorded for the carbon converted from asphalt were lower than those for the CAC. Compared with the CAC, the as-prepared carbon showed a 2.9 times higher iodine number (2047), which suggested a high surface area for the former. The activation with nitric and sulfuric acids contributed to the acidic property of the as-prepared carbon. The acetic acid-, phosphoric acid- and sulfuric acid -mediated activation of asphalt needed 3 h, 210 min, and 40–60 min , respectively. The different times required for activation was due to the strength differences of the acids. The asphalt reacted instantaneously with the nitric acid upon addition; NOx could not be observed in the final mixture. The above acid showed no AC yield. Thus, the optimal activation material was determined to be sulfuric acid (containing nitric acid at trace levels).

The influence of the acid/asphalt mass ratio on the AC yield was investigated, as shown in Figure 1A and B. As the weight ratio of acid/asphalt was increased, a clear decrease in the AC yield could be observed. In addition, the minimum time for the completion of the activation was increased with increasing weight ratio. These results suggested the evaporation of more volatile compounds out of the mixture prior to conversion. Furthermore, the cation exchange capacity (CEC) of the as-prepared carbon was also significantly influenced by the increase in weight ratio (Figure 1C). As the acid/asphalt ratio was increased to a range of 20–30, a clear increase in the CEC was observed, which subsequently showed a decreasing trend. The highest value for CEC was obtained as the acid/asphalt mass ratio reached 30. Further increase in the mass ratio led to a decreased CEC, since the high oxidation with acid caused damage to the carbon structure, as well as blocking of the mesopores and micropores by the fine carbon particles.
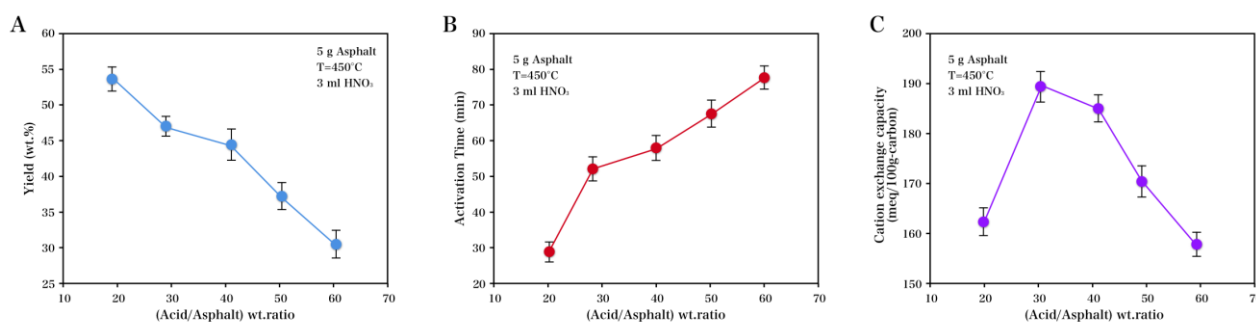
Figure 1. (A) Influence of acid/asphalt mass ratio on the production yield of AC. (B) Influence of acid/asphalt weight ratio on the activation time. (C) Cation exchange capacity of the obtained carbon from asphalt.
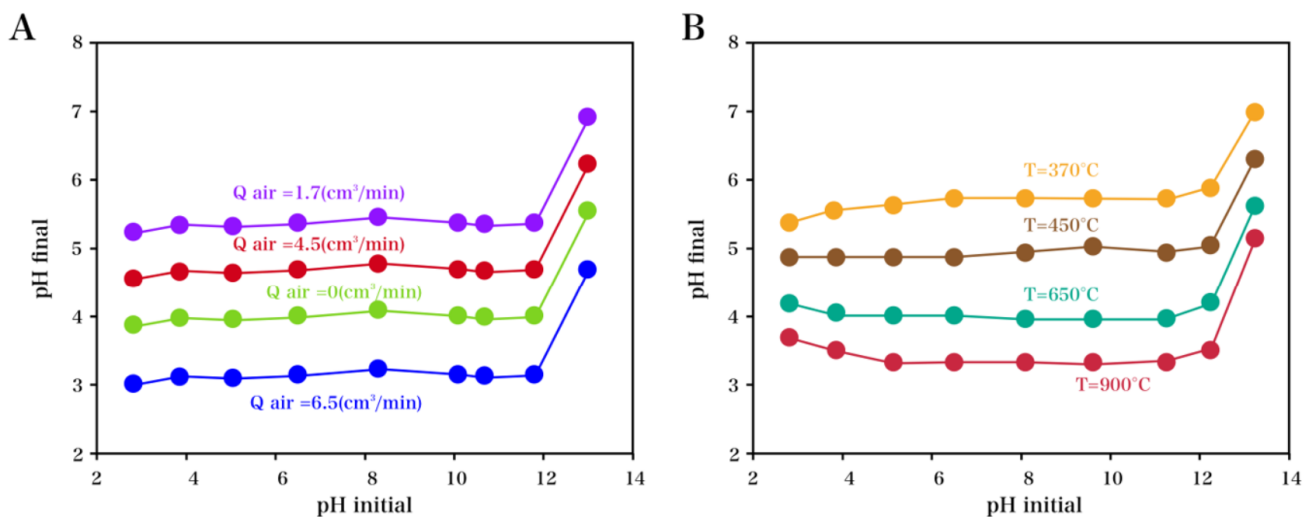
Figure 2. (A) Effect of temperature on the zero point of charge. (B) Effect of airflow rate on the zero point of charge.

The influence of temperature on the zero point of charge recorded for the as-obtained AC is shown in Figure 2A. The pH_{ZPC} was decreased from 4.17 to 2.88 with increasing activation temperature from 370 to 900 °C, possibly because the number of functional groups present on the AC surface was increased with higher activation temperature. This type of AC was confirmed as an excellent adsorbent, considering the stability of the resulting solution pH for a wide range of initial pH from 3 to 10. During the reaction, the oxidization rate of the carbon atoms was enhanced with a higher sparged airflow rate (Figure 2B), leading to an increase in the number of functional groups (largely carboxylic groups with negative charge) present on the AC surface. The elemental composition of the modified AC as determined by elemental analysis is summarized in Table 1.

Table 1. Elemental compositions of AC prepared at different temperatures.

Elemental compositions of AC (%)				
	C	H	N	O
370 °C	90.11	0.26	0.01	9.62
450 °C	96.52	0.73	0.24	2.51
650 °C	96.33	0.94	0.15	2.58
900 °C	94.57	1.41	0.25	3.77

Figure 3 shows the extent of structural order for the carbon materials measured using X-ray diffraction (XRD). For the obtained AC, a characteristic peak observed at 2 theta = 25.6° suggested high-intensity (002) diffraction, whereas diffraction peaks clearly observed at 2 theta = 42.7° and 53.2° corresponded to the (100) and (110) reflections, respectively. These results indicated that the graphitization remained at an elevated level, though the partial amorphous surface of AC was covered by layers of heteroatom-doped carbon or appended to varying oxygen-containing functional groups.
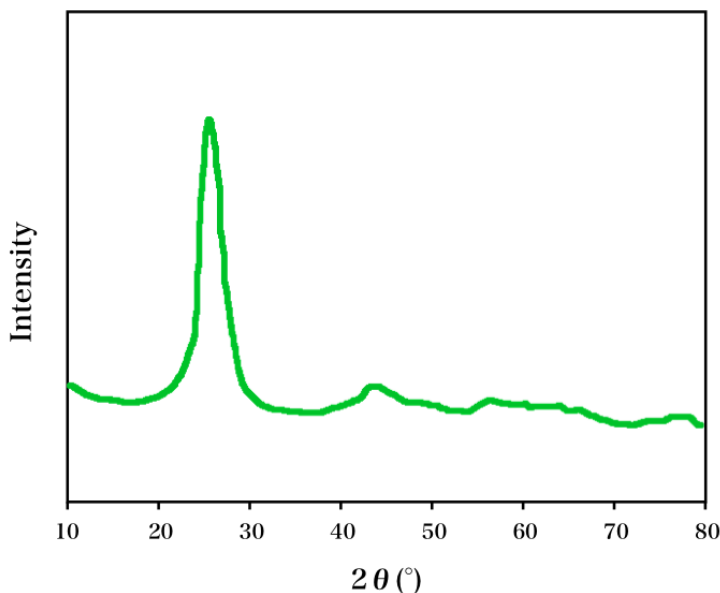
**Figure 3.** XRD diffraction pattern of the obtained AC.
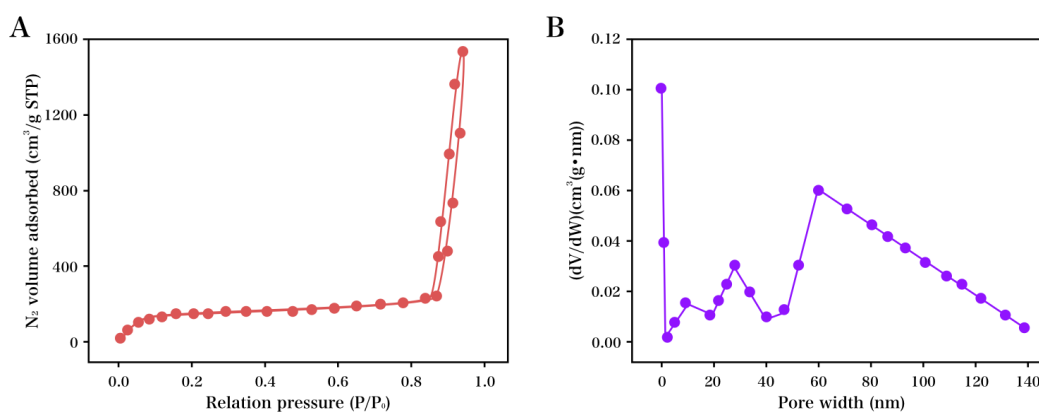
Figure 4. (A) Isotherms and (B) pore size distributions determined by nitrogen sorption of the obtained AC.

The nitrogen sorption experiments were carried out to investigate the specimen porosity. A small amount of monolayer sorption was observed when the pressure was held at a low level; at $p/p_0 > 0.9$, significant capillary condensation was measured, along with a clearly observable hysteresis loop, as shown in all the isotherms in Figure 4. These results indicated that small macropores and large mesopores were co-present with micropores, with the pore size distributions (PSDs) also providing convincing evidence for their presence. Herein, the micropore stemmed from

the inner channel of AC, which was opened via hash oxidation; therefore, the porous structure of AC was not obviously affected.

Generally, activated carbon with high specific surface area shows relatively good electrochemical catalysis property. For example, Lu [42] reported the synthesis of activated carbon with a high specific micropore surface area of 3432 m^2/g. The electrochemical measurements of the oxygen reduction reaction (ORR) were carried out to study the electrocatalytic activity of each specimen. Various methods were employed including cyclic voltammetry (CV), linear sweep voltammetry (LSV) involving a rotating disk electrode (RDE) and electron transfer number evaluation through the use of a rotating ring disk electrode (RRDE). Moreover, 0.1 M of KOH oxygen-saturated electrolyte was used throughout the experiments.
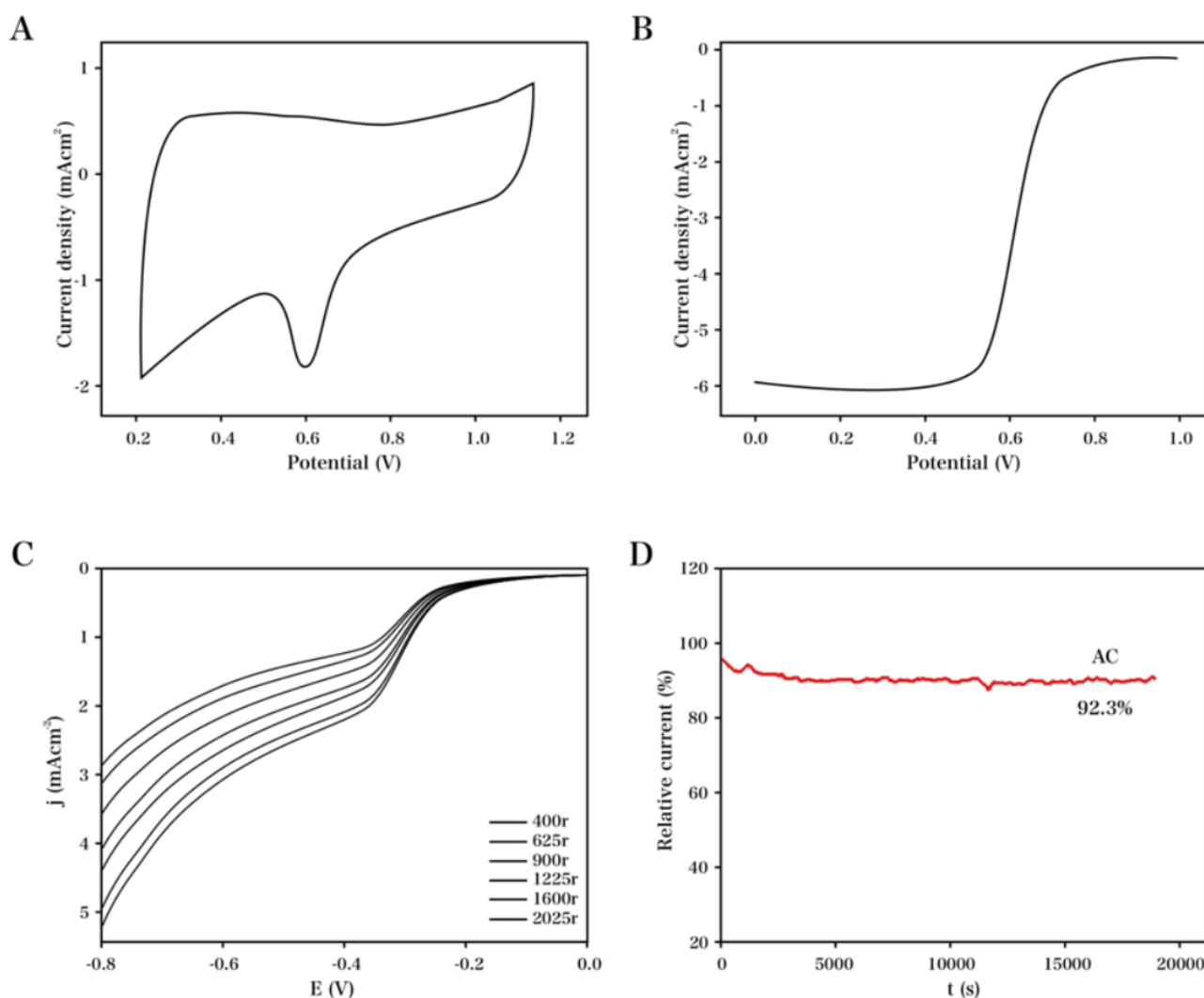
Figure 5. (A) CVs in O$_2$-saturated 0.1 M KOH, (B) comparison of the RDE polarization curves in O$_2$-saturated 0.1 M KOH at 1600 rpm. (C) RDE voltammograms for AC in an O$_2$- saturated 0.1 M aqueous KOH solution, with a scan rate of 5 mV/s at different rotation rates ranging from 400 to 2025 rpm and (D) Koutecky-Levich plot for the electrode materials at -0.3 V.

In a potential range of 0.6 V–0.8 V, oxygen reduction cathodic peaks were observed for the obtained AC (Figure 5). In addition, ORR kinetics were compared using the RDE method. For the LSV curves (Figure 5B), the parameters used were as follows: scan rate, 10 mV/s and rotating speed, 1600 rpm. At lowered overpotentials, a characteristic two-plateau peroxide pathway was shown for the obtained AC, which suggested that the selectivity of the ORR was undesirable. This result was further evidenced by the electron transfer number averaged to be 2.2 over a potential range of 0.4-0.7 V (RRDE data). The electrocatalytic properties of the AC catalyst compared to other carbon materials reported previously in the literature are shown in Table 2. Based on the results reported, AC exhibits comparable or better ORR activity compared to all other catalysts prepared previously. For further analysis of the ORR kinetics, the kinetic current density (Jk) and electron transfer number (n) were analyzed based on RDE tests conducted at various rotating speeds from 400 to 2025 rpm and the use of the K-L equations. It is observed that the current density for the ORR increases with the acceleration of the rotating speed (Figure 5C), which is due to the improved diffusion of dissolved oxygen to the surface of the modified glass carbon electrode [43].

The durability of AC toward the ORR was evaluated through chronoamperometric measurements at -0.3 V. As shown in Figure 5D, the 20000 s test only caused 7.7% activity loss on AC catalyst. This result is close to that reported for commercial Pt/C in alkaline solution [44, 45].

Table 2. Electrochemical parameters for AC compared to other catalysts for ORR.

Catalyst	E_{onset} (V)	$E_{half-wave}$ (V)	Electrolyte solution	Reference electrode	Reference
NSG700	-0.22	-0.29	0.1 M KOH	Hg/HgCl$_2$	[46]
N-S-Gas900	-0.12	-0.24	0.1 M KOH	Hg/HgCl$_2$	[47]
20% Pt/C	0.003	-0.125	0.1 M KOH	Hg/HgCl$_2$	[48]
AC	0.005	-0.122	0.1 M KOH	SCE	This work

4. CONCLUSIONS

In the present work, asphalt was successfully converted to AC powder that showed a low zero point of charge and high cation exchange capacity for a wide and stable initial pH range of 3–10. The factors affecting the AC yield included the airflow rate and/or the weight ratio for the acid/asphalt mixture. The highest CEC value was obtained for an acid/asphalt weight ratio of 30. The final AC demonstrated effective ORR active sites and remarkable performance for the electrical conductivity. Therefore, the electrochemical activity of the final AC toward ORR under alkaline conditions was comparable to that obtained for a commercial Pt/C-catalyst.

References

1. D. Nguyen-Thanh, A.I. Frenkel, J. Wang, S. O'Brien and D.L. Akins, *Applied Catalysis B Environmental*, 105 (2011) 50.

2. H.X. Yan, Z. Lan, J.Z. Wei and S.H. Chan, *International Journal of Hydrogen Energy*, 39 (2014) 8449.
3. Y. Yuan, S. Zhou and Z. Li, *Journal of Power Sources*, 195 (2010) 3490.
4. J. Liu, P. Song, M. Ruan and W. Xu, *Chinese Journal of Catalysis*, 37 (2016) 1119.
5. H. Liu, J. Liu, W. Song, F. Wang and Y. Song, *Materials Letters*, 139 (2015) 447.
6. Y. Dong and J. Li, *Chemical Communications*, 51 (2015) 572.
7. Z. Chen, H. Dong, H. Yu, H. Yu, M. Zhao and X. Zhang, *Electrocatalysis*, (2016) 1.
8. X. Zhang, Y. Chen, J. Wang and Q. Zhong, *Chemistryselect*, 1 (2016) 696.
9. Q.C. Tran, V.D. Dao, H.Y. Kim, K.D. Jung and H.S. Choi, *Applied Catalysis B Environmental*, 204 (2017) 365.
10. Z. Chen, H. Dong, H. Yu and H. Yu, *Chemical Engineering Journal*, 307 (2017) 553.
11. Y. Zhang, C. Guo, Z. Ma, H. Wu and C. Chen, *Materials*, 8 (2015) 6658.
12. Zhang, Yaqiong, Guo, Chaozhong, Ma, Zili, Wu, Huijuan, Chen and Changguo, *Materials*, 8 (2015) 6658.
13. E. Higuchi, K. Okada, M. Chiku and H. Inoue, *Electrochimica Acta*, 179 (2015) 100.
14. P. Song, Y. Zhang, J. Pan, L. Zhuang and W. Xu, *Chemical Communications*, 51 (2015) 1972.
15. H. Yano, T. Uematsu, J. Omura, M. Watanabe and H. Uchida, *Journal of Electroanalytical Chemistry*, 747 (2015) 91.
16. T. Gunji, K. Sakai, Y. Suzuki, S. Kaneko, T. Tanabe and F. Matsumoto, *Catalysis Communications*, 61 (2015) 1.
17. L. Kaluža, M.J. Larsen, M. Zdražil, D. Gulková, Z. Vít, O. Šolcová, K. Soukup, M. Koštejn, J.L. Bonde and L. Maixnerová, *Catalysis Today*, 256 (2015) 375.
18. J. Li, Y. Song, G. Zhang, H. Liu, Y. Wang, S. Sun and X. Guo, *Advanced Functional Materials*, 27 (2017) 1604356.
19. A. Jo, Y. Lee and C. Lee, *Analytica Chimica Acta*, 933 (2016) 59.
20. Y.C. Wang, Y.J. Lai, L. Song, Z.Y. Zhou, J.G. Liu, Q. Wang, X.D. Yang, C. Chen, W. Shi and Y.P. Zheng, *Angewandte Chemie*, 54 (2015) 9907.
21. M. Nunes, D.M. Fernandes, I.M. Rocha, M.F.R. Pereira, I.M. Mbomekalle, P. De Oliveira and C. Freire, *Chemistryselect*, 1 (2016) 6257.
22. J. Kang, H.M. Kim, N. Saito and M.H. Lee, *Science & Technology of Advanced Materials*, 17 (2016) 37.
23. W.H. Lee, D.W. Lee and H. Kim, *Journal of the Electrochemical Society*, 162 (2015) F744.
24. Y. Xiao, J. Ge, M. Xiao, V. Fateev, C. Liu and W. Xing, *Electrochimica Acta*, 209 (2016) 551.
25. E.N. Alvar, B. Zhou and S.H. Eichhorn, *Journal of Materials Chemistry A*, 4 (2016) 6540.
26. Y. Qiu, L. Xin, F. Jia, J. Xie and W. Li, *Langmuir the Acs Journal of Surfaces & Colloids*, 32 (2016) 12569.
27. Z. Qi, H. Dong, H. Yu, M. Zhao and H. Yu, *Journal of Cleaner Production*, (2017)
28. A. Mikolajczuk-Zychora, A. Borodzinski, P. Kedzierzawski, B. Mierzwa, M. Mazurkiewicz-Pawlicka, L. Stobinski, E. Ciecierska, A. Zimoch and M. Opałło, *Applied Surface Science*, 388 (2016) 645.
29. O. Akira, T. Yuta, O. Toshikazu, T. Shotaro, S. Akira and H. Takashi, *Journal of Porphyrins & Phthalocyanines*, 19 (2015)
30. W. Shi, Y.C. Wang, C. Chen, X.D. Yang, Z.Y. Zhou and S.G. Sun, *Chinese Journal of Catalysis*, 37 (2016) 1103.
31. L. Li, Q. Li, B. Noffke and K. Raghavachari, *Electrochemical Society*, (2015)
32. P. Liu, J. Kong, Y. Liu, Q. Liu and H. Zhu, *Journal of Power Sources*, 278 (2015) 522.
33. J. Kim, J.S. Jang, D.H. Peck, B. Lee, S.H. Yoon and D.H. Jung, *Nanomaterials*, 6 (2016) 148.
34. J. Liu, P. Song, Z. Ning and W. Xu, *Electrocatalysis*, 6 (2015) 132.
35. J.F. Carneiro, R.S. Rocha, P. Hammer, R. Bertazzoli and M.R.V. Lanza, *Applied Catalysis A General*, 517 (2016) 161.

36. H. Erikson, A. Sarapuu, K. Tammeveski, J. Solla‐Gullón and J.M. Feliu, *Chemelectrochem*, 1 (2015) 1338.
37. A. Marcilla, S. García-García, M. Asensio and J.A. Conesa, *Carbon*, 38 (2000) 429.
38. A.H. El-Sheikh, A.P. Newman, H.K. Al-Daffaee, S. Phull and N. Cresswell, *Journal of Analytical and Applied Pyrolysis*, 71 (2004) 151.
39. R.-L. Tseng and S.-K. Tseng, *Journal of Colloid and Interface Science*, 287 (2005) 428.
40. A.M. Youssef, N.R.E. Radwan, I. Abdel-Gawad and G.A.A. Singer, *Colloids and Surfaces A: Physicochemical and Engineering Aspects*, 252 (2005) 143.
41. M.F.R. Pereira, S.F. Soares, J.J.M. Órfão and J.L. Figueiredo, *Carbon*, 41 (2003) 811.
42. L. Wei, M. Sevilla, A.B. Fuertes, R. Mokaya and G. Yushin, *Advanced Functional Materials*, 22 (2012) 827.
43. X.-K. Kong, C.-L. Chen and Q.-W. Chen, *Chemical Society Reviews*, 43 (2014) 2841.
44. K. Qu, Y. Zheng, S. Dai and S.Z. Qiao, *Nanoscale*, 7 (2015) 12598.
45. Z. Liu, H. Nie, Z. Yang, J. Zhang, Z. Jin, Y. Lu, Z. Xiao and S. Huang, *Nanoscale*, 5 (2013) 3283.
46. F. Pan, J. Jin, X. Fu, Q. Liu and J. Zhang, *ACS applied materials & interfaces*, 5 (2013) 11108.
47. X. Wang, J. Wang, D. Wang, S. Dou, Z. Ma, J. Wu, L. Tao, A. Shen, C. Ouyang and Q. Liu, *Chemical communications*, 50 (2014) 4839.
48. S. Meng, M. Yu, J. Liu and S. Li, *Int. J. Electrochem. Sci*, 12 (2017) 5404